Gain spectra of 1.3 μm GaInNAs laser diodes

Zhang, X.; Gupta, J. A.; Barrios, P. J.; Pakulski, G.; Wu, X.; Delâge, A.

Publisher's version / Version de l'éditeur:
https://doi.org/10.1116/1.2186662
Journal of vacuum science and technology A, 24, 3, pp. 787-790, 2006-05

Gain spectra of 1.3 μm GaInNAs laser diodes

X. Zhang
Institute for Microstructural Sciences, National Research Council of Canada, Ottawa, Ontario K1A 0R6, Canada and Centre for Research in Photonics, University of Ottawa, Ottawa, Ontario K1N 6N5, Canada

J. A. Gupta,[a] P. J. Barrios, G. Pakulski, X. Wu, and A. Delâge
Institute for Microstructural Sciences, National Research Council of Canada, Ottawa, Ontario K1A 0R6, Canada

(Received 7 September 2005; accepted 13 February 2006; published 4 May 2006)

We present an experimental investigation of the optical gain properties of 1.3 μm GaInNAs double quantum well ridge waveguide laser diodes. High-resolution gain spectra versus injection current and temperature were obtained by measuring the modulation depth introduced into the spontaneous emission spectrum by the Fabry-Pérot resonances. As the injection current increases, the modal gain spectral peak experiences a small blueshift over the photon energy, and the magnitude increases asymptotically, saturating at the lasing threshold level of 24.4 cm^{-1}. The peak of the modal gain spectra exhibits a redshift with an average rate of 0.58 nm/°C as the temperature increases from 30 to 50 °C. For wavelengths corresponding to photon energy below the band gap, the modal gain spectra converge to the internal loss of 7 cm^{-1}. The full width at half maximum of the gain spectrum is 41.1 meV at 30 °C, 40 mA and increases with injection current at a rate of 0.42 meV/mA. The high optical gain and low internal loss indicate that GaInNAs is a promising active material for long wavelength laser diodes. © *2006 American Vacuum Society.* [DOI: 10.1116/1.2186662]

I. INTRODUCTION

Cost pressures in the data communication industry have recently provided a tremendous impetus for the development of coolerless 1.31–1.55 μm semiconductor laser diodes which can be modulated up to 10 GHz. Traditionally, InGaAsP quantum wells (QWs) grown on InP substrates have been used to meet these wavelength requirements. However, InGaAsP QWs are intrinsically sensitive to temperature. Additional electronics are needed to maintain temperature stability, resulting in substantial packaging costs. Thus, other material systems have been intensively investigated for improving the laser temperature characteristics. The candidates include AlInGaAs–InP (Ref. 1) and GaInNAs–GaAs.[2,3] Both systems have a large conduction band offset between the QWs and barriers. This large band offset provides better electron confinement that suppresses thermal-induced carrier leakage, enhances differential gain, and reduces the temperature sensitivity of the devices.

Unlike conventional III-V semiconductor alloys, the properties of GaInNAs cannot be reasonably interpolated among the binary compounds and GaInNAs QWs have a remarkably large electron mass, which results from adding even a small amount of nitrogen into ternary GaInAs.[4] The overlap between electrons and holes is increased due to the closer match in effective masses, resulting in a more efficient radiative recombination. Moreover, GaInNAs can be grown coherently on GaAs substrates, enabling the fabrication of vertical cavity surface emitting lasers (VCSELs) based on the high refractive index contrast of AlGaAs/GaAs Bragg reflectors.[5]

In this article, we present the gain properties of a high efficiency, low threshold current double quantum well (DQW) GaInNAs ridge waveguide (RWG) laser grown on GaAs by molecular beam epitaxy (MBE). The high-resolution gain spectra over a set of subthreshold currents and temperatures were extracted by measuring the amplified spontaneous emission (ASE) spectra of the laser. The features of the gain spectrum were analyzed and compared to the other conventional material systems. The transparency current, internal loss, and model gain were extracted. The results reaffirm the potential of GaInNAs as a promising light source for optical communication systems at 1.3 μm and beyond.

II. DEVICE FABRICATION

The 1.3 μm GaInNAs lasers were grown on an *n*-type GaAs (100) substrate in a custom VG V90 MBE system using conventional effusion cells for Ga, In, and Al with As_2 generated by a valved cracker cell. A Veeco UniBulb radio frequency (rf) plasma cell was used to produce active nitrogen using Ar/N_2 dynamic gas switching.[6] The active region of the laser diode is composed of two 6.7 nm $Ga_{0.67}In_{0.33}N_{0.015}As_{0.985}$ quantum wells separated by a 20 nm GaAs barrier. Two additional 148 nm GaAs layers above and below the quantum wells complete the waveguide. The *n*-type cladding consists of a 1.8 μm $Al_{0.33}Ga_{0.67}As$:Si layer, grown as a (97 nm AlGaAs:Si/3 nm GaAs:Si) superlattice, where the thin GaAs layers were inserted to promote a smoother surface. The *p*-type cladding layer is 1.5 μm *p*-$Al_{0.33}Ga_{0.67}As$ doped with Be. The doping concentrations are 2.0×10^{18} and 1.0×10^{18} cm^{-3} for the *n*-type and *p*-type layers, respectively. A 200 nm heavily doped (1.0

[a]Electronic mail: james.gupta@nrc-cnrc.gc.ca

$\times 10^{19}$ cm^{-3}) GaAs:Be layer was grown as the top contact. Before device fabrication the wafer was annealed at 775 °C for 5 min in a flowing N_2 ambient with GaAs proximity capping. RWG lasers were fabricated using inductively coupled plasma reactive ion etching (ICP-RIE). TiPtAu and NiGeAu metallizations were used for the *p*-type and *n*-type contacts, respectively. The lasers were cleaved into 448 μm long Fabry-Pérot (FP) cavities and mounted *p* side up onto alumina carriers.

III. MEASUREMENT

To extract gain spectra, the ASE from the laser was measured using an Ando AQ6317B optical spectrum analyzer (OSA) with a 0.1 nm resolution bandwidth. A polarization maintaining fiber with a tapered tip couples the laser output directly from the laser facet. Careful adjustment of the fiber position leads to a high coupling efficiency of 20%. The modal gain was determined using the Hakki-Paoli method.[7] With the laser biased below threshold, the FP resonance of the laser cavity induces intensity modulations in the spontaneous emission. As carriers pump the active material, the modulation depth increases. By measuring and analyzing the depth of modulation $r(\lambda)$ between the peaks and valleys of the ASE spectrum, the modal gain spectrum can be obtained using the following equation:

$$\Gamma g = \frac{1}{L}\ln\left(\frac{\sqrt{r(\lambda)}+1}{\sqrt{r(\lambda)}-1}\right)+\frac{1}{L}\ln R, \tag{1}$$

where Γ is the confinement factor, L is the cavity length, and R is the reflectivity of the laser facets.

The net modal gain $g_{\text{net}}=\Gamma g-\alpha_i$ can be calculated by subtracting the internal loss α_i from the modal gain Γg. The material gain g can be deduced once the confinement factor Γ is calculated by a conventional mode solver.

Before the ASE spectral measurements, the temperature dependence of the lasing wavelength was measured by biasing the laser just above threshold at each temperature. The longitudinal mode spacing $\Delta\lambda$ for each temperature at the lasing wavelength was accurately measured using the OSA for the calculation of the modal index n_{eff} based on the FP resonance condition $\Delta\lambda=\lambda^2/2Ln_{\text{eff}}$. The facet reflectivity was obtained from $R=((n_{\text{eff}}-1)/(n_{\text{eff}}+1))^2$. For the 448 μm long device, the measured mode spacing was 0.495 nm at the 10 °C lasing wavelength of 1276 nm and the facet reflectivity was 0.327. The modal index changes with wavelength. However, the change in facet reflectivity over the 100 nm measurement span was neglected. This induces a less than 1 cm^{-1} error, which is normally negligible, at the low energy side of the extracted gain spectra.

A narrow ridge, short cavity laser that operates with a single transverse mode was used for an accurate modal gain extraction below −60 dB. The monotonous ripple envelope from the single mode enables an automated computer program to read the ripple contrast reliably. Moreover, shorter devices are more suitable for obtaining smooth spectra with the resolution of this OSA. Both factors are particularly important for low subthreshold current measurements at the high photon energy side of the gain spectra.

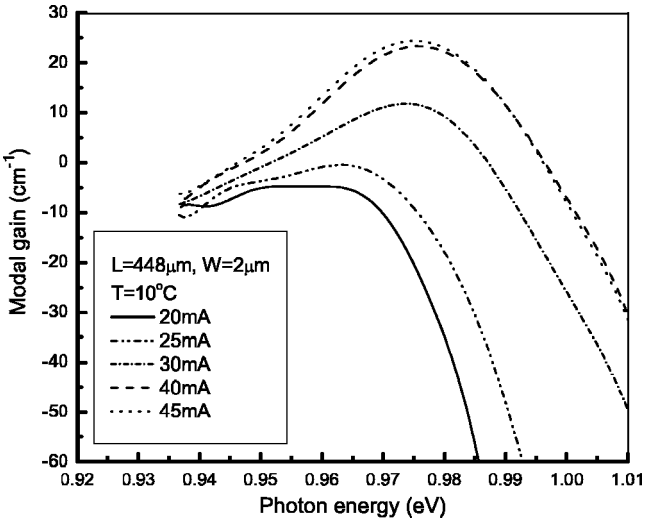

FIG. 1. Subthreshold modal gain spectra measured at 10 °C. The biasing currents are indicated.

IV. RESULTS

Figures 1–3 show the modal gain spectra as a function of photon energy for a 2×448 μm^2 device at different subthreshold driving currents measured at 10, 30, and 50 °C, respectively. For all temperatures, the overall intensity of the gain spectra increases with injection current. However, the gain increases more at the high photon energy side of the spectra. At the low photon energy side, the gain spectra converge to the internal loss α_i. In this device, the internal loss was found to be approximately $\alpha_i=7$ cm^{-1} and was independent of temperature. The 24.4 cm^{-1} peak modal gain at the lasing threshold marks the mirror loss. This value is in a

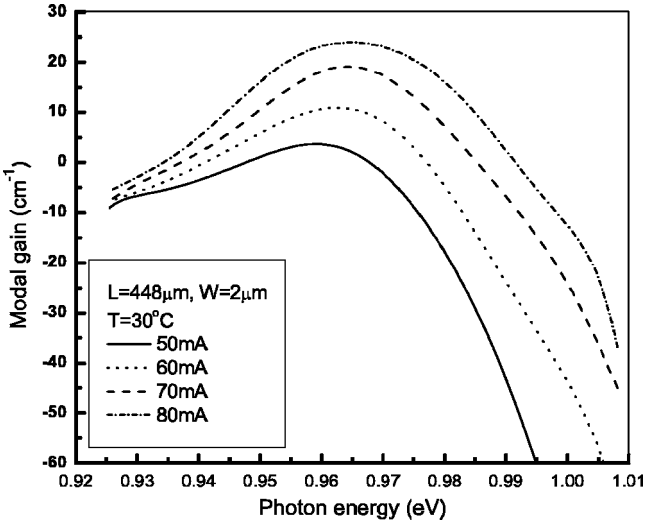

FIG. 2. Subthreshold modal gain spectra measured at 30 °C. The biasing currents are indicated.

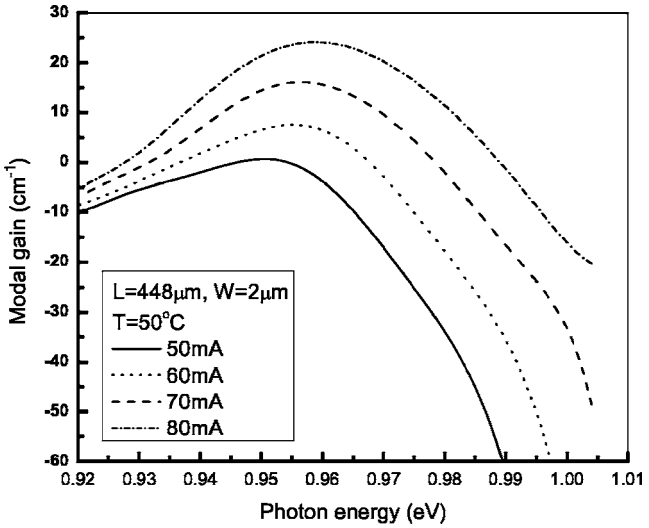

FIG. 3. Subthreshold modal gain spectra measured at 50 °C. The biasing currents are indicated.

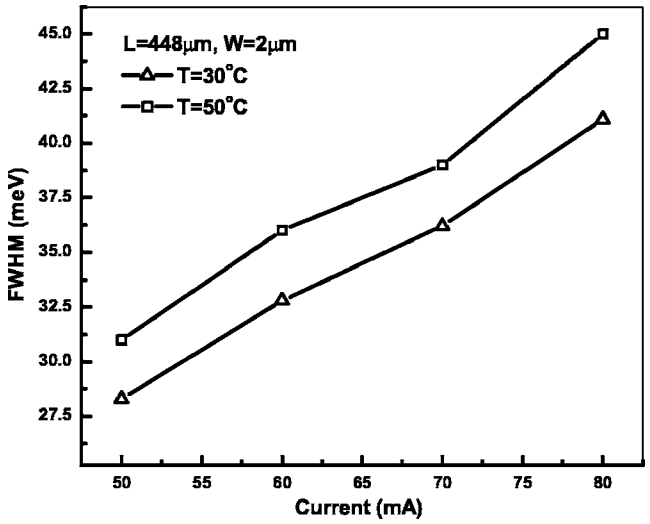

FIG. 5. FWHM of the gain spectra as a function of subthreshold current measured at 30 and 50 °C.

good agreement with the calculated mirror loss of 25.0 cm^{-1}, using $\alpha_m=(1/L)\times Ln(1/R)$ and the facet reflectivity described above.

The transparency current can also be estimated using Fig. 1 from the value of the bias current at which the gain spectrum crosses the value of zero net modal gain. At 10 °C, the laser experiences stimulated emission at 1276 nm (972 meV), yielding a transparency current of 24 mA. This current includes the lateral leakage current through the *p*-type cladding layer in the RWG laser structure. Thus, it overestimates the transparency current. To determine the lateral leakage current, the threshold current dependence on ridge width was measured using a set of devices with different widths and equal cavity lengths using the method of Ref. 8. In this way the lateral leakage current was determined to be 17 mA and the estimated transparency current is 7 mA.

Figure 4 shows the peak net modal gain as a function of subthreshold current measured at 10 and 30 °C, respectively.

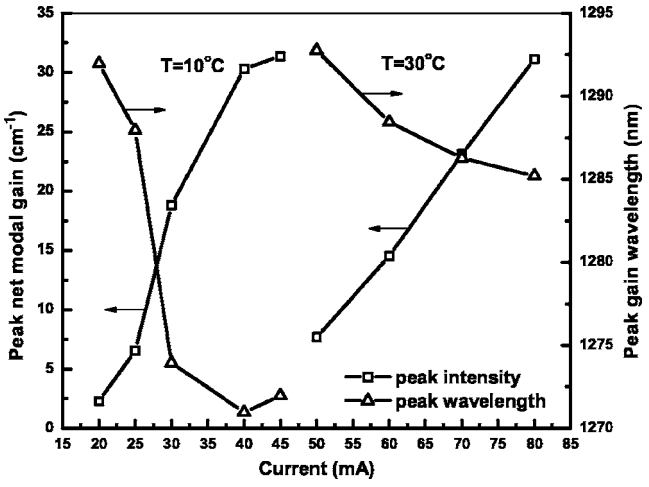

FIG. 4. Peak net modal gain and wavelength as a function of subthreshold current measured at 10 and 30 °C.

The peak net modal gain increases asymptotically and saturates at the threshold value of 31.4 cm^{-1}. Due to the carrier recombination for stimulated emission, the gain clamps at this value when the bias current exceeds the threshold. The confinement factor Γ was calculated to be 0.032 using the mode solver LAS2D. Thus the material gain g is estimated to be about 1000 cm^{-1}. This value is only slightly lower than the theoretical result ($\sim$1300 cm^{-1}) for 1.3 μm GaInNAs quantum wells.[3] On the other hand, the differential gain dg/dI is 1.25 cm^{-1}/mA at 10 °C and decreases with increasing temperature. This value is lower than the typical 5 cm^{-1}/mA in the InGaAs(P)/InP system.[9] However, it is comparable to the value of 1.9 cm^{-1}/mA measured in AlGaInAs/InP lasers.[10]

The peak wavelength of modal gain as a function of subthreshold current is also plotted in Fig. 4. The usual blueshift of the maximum gain over the bias current is observed, where the average rate of the shift is -0.25 nm/mA. Compared to the strong blueshift of -1 nm/mA to -3 nm/mA in 1.3 μm AlGaInAs–InP, InGaAsP–InP, and highly strained InGaAs–GaAs QW structures,[9–11] these GaInNAs/GaAs QWs exhibit a weaker band filling effect.

Figure 5 depicts the full width at half maximum (FWHM) of the gain spectra as a function of subthreshold current measured at 30 and 50 °C, respectively. The variation of the FWHM can be approximated by a linear dependence on the bias current at a rate of 0.42 meV/mA, reaching a value of 41.1 meV at the lasing threshold at 30 °C. The spectra are consistently broader at 50 °C. However, the linear dependence is approximately independent of temperature. A similar effect was reported for a 1.3 μm GaInAsP/InP multiquantum-well (MQW) laser[9] with a comparable FWHM (about 40 meV at 25 °C). However, the FWHM of the GaInAsP/InP laser increases at a much larger rate (in a range of 2–3 meV/mA) with bias current. In addition to the weak blueshift of the peak gain described above, the small spectral broadening over the injection current indicates that the

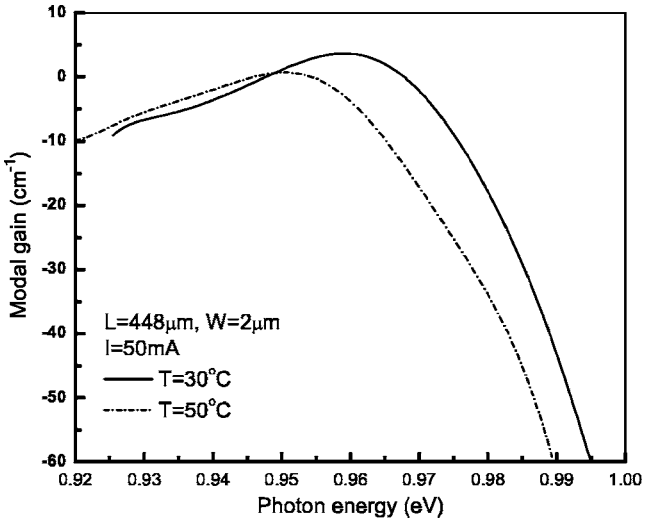

FIG. 6. Modal gain spectra measured at 50 mA, 30 and 50 °C, respectively.

GaInNAs QWs have a small band filling effect with increasing carrier injection, pointing to a larger density of states than the conventional III-V compounds. The large density of states in the QWs could be explained by the unique nonparabolic band structure in GaInNAs, where the electron mass increases dramatically over the split energy states.

Figure 6 presents the temperature dependence of the gain spectra. At a constant biasing current of 50 mA, the wavelength of the peak modal gain increases with temperature at an average rate of 0.58 nm/ °C over this 20 °C interval. This result is similar to the InP-based and highly strained InGaAs–GaAs materials, in which the peak modal gain increased at rates of 0.3–0.5 nm/ °C.[9–11] The significant redshift of the peak modal gain is associated with the temperature-induced band gap shrinkage. Beside the redshift, the peak modal gain decreases at an average rate of -0.15 cm^{-1}/ °C as the temperature increases over this 20 °C interval. Compared to the typical value of about -0.3 cm^{-1}/ °C,[9–11] the sensitivity of gain over temperature is in the same order of magnitude as in 1.3 μm AlGaInAs–InP and InGaAsP–InP QW structures.

V. CONCLUSIONS

Extensive experimental characterization of 1.3 μm DQW RWG GaInNAs/GaAs laser has been used to investigate the temperature and current dependences of the optical gain properties. The results indicate that GaInNAs is a competitive material system with InGaAsP–InP and AlGaInAs–InP in terms of internal loss, transparency current, and optical gain. Moreover, a small band filling effect with increasing carrier injection provides a further indication of the remarkable uniqueness of the band structure of GaInNAs QWs.

[1] S. R. Selmic, T. Chou, J. Sih, J. B. Kirk, A. Mantie, J. K. Butler, D. Bour, and G. A. Evans, IEEE J. Sel. Top. Quantum Electron. **7**, 340 (2001).
[2] M. Kondow, T. Kitatani, S. Nakatsuka, M. C. Larson, K. Nakahara, Y. Yazawa, M. Okai, and K. Uomi, IEEE J. Sel. Top. Quantum Electron. **3**, 719 (1997).
[3] S. Tomic *et al.*, IEEE J. Sel. Top. Quantum Electron. **9**, 1228 (2003).
[4] C. Skierbiszewski *et al.*, Appl. Phys. Lett. **76**, 2409 (2000).
[5] A. W. Jackson *et al.*, Electron. Lett. **37**, 355 (2001).
[6] J. A. Gupta *et al.*, J. Cryst. Growth **242**, 141 (2002).
[7] B. W. Hakki and T. L. Paoli, J. Appl. Phys. **46**, 1299 (1975).
[8] S. Y. Hu, D. B. Young, A. C. Gossard, and L. A. Coldren, IEEE J. Quantum Electron. **30**, 2245 (1994).
[9] D. A. Ackerman, G. E. Shtengel, M. S. Hybertsen, P. A. Morton, R. F. Kazarinov, T. Tanbun-Ek, and R. A. Logan, IEEE J. Sel. Top. Quantum Electron. **1**, 250 (1995).
[10] T. J. Houle *et al.*, IEEE J. Quantum Electron. **41**, 132 (2005).
[11] S. Mogg, N. Chitica, R. Schatz, and M. Hammar, Appl. Phys. Lett. **81**, 2334 (2002).